Experimental Assessment and Modeling of Losses in Interlocked Magnetic Cores

Experimental Assessment and Modeling of Losses in Interlocked Magnetic Cores

Silvio Vaschetto, *Senior Member, IEEE*, Zbigniew Gmyrek, Christoph Dobler, *Student Member, IEEE*, Gerd Bramerdorfer, *Senior Member, IEEE,* Andrea Cavagnino, *Fellow, IEEE*

Abstract— **The use of interlocks often represents an affordable stacking solution for soft magnetic cores in mass production of electrical machines. However, due to the process itself, the material behavior and thus the resulting electrical machine performance is negatively impacted. On the one hand, this is due to additional conductive paths, which increase the eddy current losses. On the other hand, locally introduced mechanical stresses occur. These lead to non-negligible degradation of the magnetic material properties inside and around the interlock area, following higher hysteresis losses. This study investigates and develops a reliable and accurate three-dimensional FEM model that considers the contact resistance between interlocks and laminations, as well as layered regions for the material degradation around the interlock area. Examples of flux and eddy current density distributions are provided, together with the computation of the total iron losses for a variable number of rectangular dowels in the yoke of stator core samples. The numerical analyses are validated by several interlaboratory measurements conducted on multiple stator core samples made of two different grades of electrical steels and with different numbers of interlocks. Results reveal impact of some percent on the core losses and well evident degradation on the material *BH* curve.**

***Index Terms* — 3D FEM, eddy currents, forming process, magnetic cores, material deterioration, interlock dowels, iron losses.**

I. Introduction

In the field of electric machines and drives technology, the improvement of existing modeling methods as well as the development of new modelling approaches is an essential core area of research. Particularly, machine topologies, material models and manufacturing processes are constantly being examined and improved [1]. Nowadays, engineering tools such as Finite Element Method (FEM) are used to calculate and optimize electric machine designs [2]. To enhance the accuracy of the predicted machines performance these tools require for accurate data on the materials used for the machine realization [3], [4]. Of particular interest is the magnetization behavior and the loss characteristic of soft magnetic materials. In fact, it is well known that certain steps in the production chain of lamination sheets for electrical machines have a negative impact on the soft magnetic materials performance [5]-[9]. Therefore, great effort is made to characterize and model the influence of manufacturing steps on the materials magnetizing and loss behavior and thus the resulting motor design performance [10], [11]. In high production volumes of magnetic cores for electrical machines, the progressive stacking die is the usual forming solution. Those stacks are assembled using different techniques, such as clamping, welding, full-face bonding or by the use of interlocks. Any of these assembly methods show certain advantages and disadvantages. For instance, the full-face bonding has the least impact on the magnetization behavior of the soft magnetic material, but it is certainly one of the more complex techniques, which is reflected in the resulting costs [7]. In case of welding, the stack of laminations is held together by one or multiple welding seams along the axial direction of the machine. This process introduces thermal and mechanical stress in the material, which results in a degradation of the magnetic material. Furthermore, the weld seams are electrically conductive and therefore lead to almost perfect short circuits between the individual laminated layers, with consequent high eddy current effects [7]-[10].

The stacking process of magnetic cores through interlocks is realized stamping and staking the lamination directly in the die system. In particular, the lamination sheets are clamped together by means of dowels that have to ensure the mechanical strength of the magnetic core. While interlocking is a reasonably priced technology, there are disadvantages to be accounted for. Due to the mechanical alteration of the materials morphology, local deterioration of the magnetic material in the dowel regions, and parasitic electrical contacts between subsequent laminations are being introduced. These undesirable effects in turn contribute to increased iron losses of the core material. Analyzing the available literature, it is possible to conclude that as of yet there is not a comprehensive solution to the problem of interlocks impact on the magnetization characteristics of the finished core, as well as an estimation of the loss increase.

Manuscript received November 23, 2021; revised January 24, 2022; accepted March 11, 2022. Paper 2021-EMC-1226.R1, presented at the 2020 IEEE Energy Conversion Congress and Exposition, Online Edition, Oct.. 11–Oct. 15, and approved for publication in the IEEE TRANSACTIONSON INDUSTRY APPLICATIONS by the Electric Machines Committee of the IEEE Industry Application Society. (Corresponding author: Silvio Vaschetto.).
S. Vaschetto and A. Cavagnino are with the Politecnico di Torino, Dipartimento Energia "G. Ferraris", Torino, 10129, Italy (e-mail: silvio.vaschetto@polito.it, andrea.cavagnino@polito.it,).
Z. Gmyrek is with the Institute of Mechatronics and Information Systems, Lodz University of Technology, Lodz, Poland (e-mail: zbigniew.gmyrek@p.lodz.pl).
C. Dobler and G. Bramerdorfer are with Institute of Electrical Drives and Power Electronics, Johannes Kepler University Linz, Linz, Austria (e-mail: christoph.dobler@jku.at, gerd.bramerdorfer@jku.at).
Color versions of one or more of the figures in this article are available online at https://ieeexplore.ieee.org. Digital Object Identifier XXXXXX

The aim of this research study is to model the presence of interlock dowels by means of FEM models, that also consider the magnetization characteristic worsening, to accurately predict the iron losses increase in interlocked magnetic stator cores of ac machines. In particular, the investigation extends the activities originally presented in [1], further elaborating and conducting several experimental measurements both on M270-50A and M400-50A fully processed magnetic materials. To enhance the accuracy of the numerical estimations and the confidence on the proposed modeling techniques, dedicated stator core samples with variable number of interlocks have been produced and tested. The tests were performed at different supply frequencies and magnetic induction values up to the material magnetic saturation. The results trustworthiness has been proved through a round robin test procedure, consisting in multiple tests performed by two independent laboratories, also using slightly different measurement approaches.

II. Literature review

Although the materials degradation due to the interlock process is less investigated than other machining and assembly processes, it is worth to mention that some interesting studies have already been presented in literature.

In [12], five small toroidal samples made of M330-35A interlocked laminations are analyzed through a 3D FEM model that also considers the insulation between each sheet. The analyses focus on the distribution of eddy currents in the interlock regions for a magnetizing frequency of 400 Hz. This model assumes a perfect electrical contact between the laminations due to the interlocks. Furthermore, the magnetic permeability is set to a constant value for the model, hence the material deterioration due to the manufacturing process was not accounted for. In [13], the focus of investigation lies again on small interlocked toroidal samples. These specimens are made of M400-50A. Measurements on samples with different number of interlocks and different number of stacked laminations are carried out at 50 Hz, creating a database of results useful for modeling. In [14], measurements in the range 100-400 Hz are performed to assess the interlocks influence on the properties of 50CS1300JIS laminations with rectangular and circular dowels.

In [15] a 3D FEM model of core fragments is presented together with a complete 2D model of an interlocked induction motor. The study considers the contact resistance between the steel sheets due to the interlocks, as well as the degradation of the magnetic properties in the interlock area due to the manufacturing process. However, the materials degradation in the affected regions has been considered imposing a priori estimated permeability equal to 2/3 of that for the unaffected material, but no experimental validations are reported.

In [16], one of the most complete experimental research works on the effects of rectangular interlock dowels is presented. In detail, the analysis is conducted on small toroidal samples made of 35JNE250 electrical steel, with different dowel positioning as well as with a varying number of interlock connections. The presented data can be used to simulate the effects of interlocks on the iron losses, but a detailed modeling procedure is not reported.

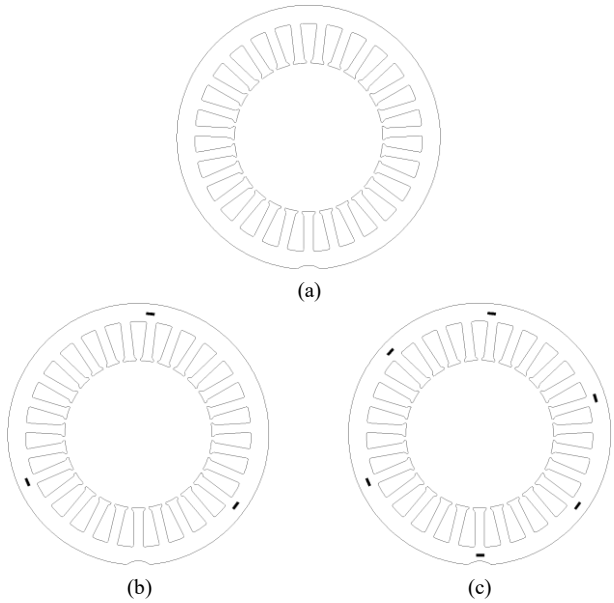

Fig. 1: The stator samples with zero (a), three (b) and six (c) interlocks.

III. The Stator Samples Construction

The shape of the samples used for the experimental characterization of soft magnetic materials basically depends on the considered measurement technique [17]. The most frequently used techniques are those based on the induction principle. Also, existing methods using said principle mainly differ on the samples shape. Broadly employed in industry is the Epstein Frame. This is due to the easy sample preparation: the measuring and the sensing coil are premade and can be used on multiple samples with minimal additional effort. Unfortunately, this method exhibits non beneficial effects in the corner zones of the frame, especially when characterizing at high frequency values. Another frequently applied device is the single sheet tester. Also in this case, the samples preparation time is quite low due to the open nature of the geometry in use; however, an additional yoke is required.

Another characterizing technique resorts to the use of ring shaped (toroidal) specimens. Due to the closed geometry, the samples preparation is the most time consuming compared to the other methods. However, the toroid circular shape results in a sample magnetization similar to that in laminations of rotating electrical machines. For this reason, this characterizing technique has been considered for this research activity.

In [18]-[20] details are discussed concerning the technological process of high-speed stamping and interlocking of laminations. In particular, [20] focuses on the contact interference between circular interlocks and laminations. However, even if some information is available in literature, it is necessary to produce and test ad-hoc stator core specimens to collect the data required to calibrate and validate the FEM models presented in the next sections. In literature, small interlocked toroidal samples having variable number of dowels are often adopted due to the '*limited*' cost of their progressive die. For this research project, commercially available interlocked stator cores have been selected. The authors requested the company to modify the existing die in order to produce stator samples with zero, three, and six interlocks along the average circumference of the yokes, as illustrated in Fig. 1.

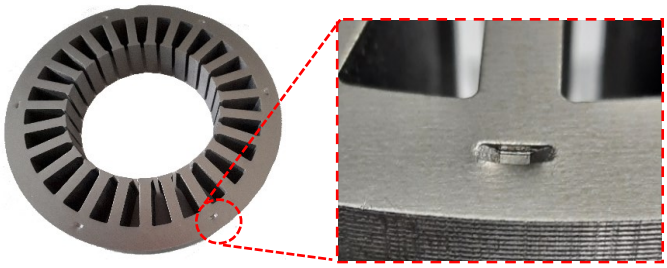

Fig. 2: Magnetic core sample and detail of the used interlocks shape.

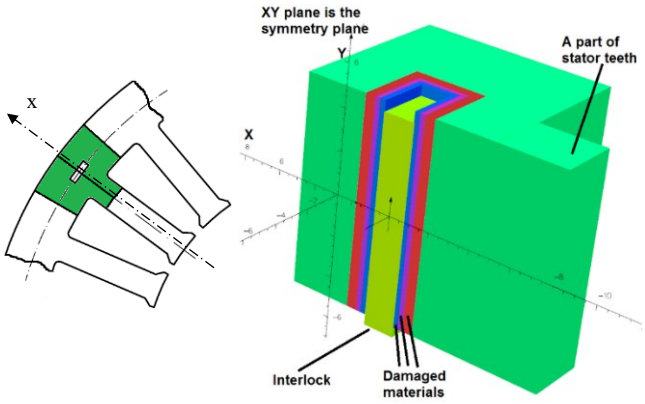

Fig. 3:The modeled region (green, on the left) and half of the domain showing the presence of zones of differently damaged magnetic material (on the right).

The yoke diameter where the dowels are stamped is 148 mm, while the yoke radial thickness is 11 mm, and the axial length of the core is 30 mm. The weight of the yoke element, evaluated by the specific gravity, is approximately 1.1 kg.

To measure the magnetizing characteristic and the iron losses in the yokes, each stator core is wound as a toroidal sample for the experimental activity (i.e., a sensing winding, wound as close as possible to the yoke, and a magnetizing winding) [21]. This practical measurement approach is mostly considered as a good cost-benefit tradeoff for magnetic and energetic studies on stator cores for electrical machines. For instance, the same measurement approach has been used in [22] to investigate the temperature impact on non-oriented steel laminations. Figure 2 shows a sample of the investigated stator cores, together with a detail of the interlocks shape. The dimensions of the rectangular interlock dowel are 1.5x5mm, while its depth is approximately equal to the thickness of the lamination.

The production of a limited number of samples for research activity purposes is not a straightforward operation for a company that produces stator cores in series for electric machine manufacturers. In fact, it is required to stop many times the production line, open the progressive stacking die to change the number of interlock punches and then reassemble it. Therefore, willing to investigate two different magnetic materials and three interlock configurations (zero, three, and six, respectively), three sets of six samples each have been produced. Among these three sets, two were intended for magnetic/energetic assessments performed in two independent laboratories to confirm the measurements repeatability, while the third one is intended for future research activities, such as the experimental investigation of the annealing impact in interlocked samples.

The experimental results included in this paper were obtained for the interlocked core samples made of the M270-50A, as well as the M400-50A magnetic material. The initial calibration of the FEM models, both for the '*degraded*' and '*healthy*' regions, have been done using magnetization curves and specific loss trends measured by the authors in previous research activities on M270-50A and M400-50A materials subjected to the punching process [9].

IV. 3D-FEM Model for the Interlocked Magnetic Stator Core

With increasing number of '*a priori*' simplifications and assumptions, the reliability of the FEM results decreases significantly. Often, 2D models are used to quantify the interlock effects; however, these bi-dimensional analyses are based on specific assumptions and the results have limited generality, being strongly dependent on the considered problem. Even though a 3D FEM requires more computational resources, for this research activity the authors decide to use this modeling approach to reduce as much as possible the number of simplifications.

Thanks to the authors' experience in the modeling of damaged material caused by several forming processes of the stator core, and after several attempts to get reasonable and physical results, the 3D-FEM model shown in Fig. 3 is proposed. To limit the computation time, only the green fragment shown in the figure has been considered. This is possible because in the tested samples the magnetizing winding is wound around the stator yoke, limiting to this stator portion the path for the magnetic flux. The axial thickness of the modeled domain is nearly 9.5 mm that correspond to 18 insulated laminations. For this fragment of the total volume, approximately 500,000 elements must be used to have an appropriately dense mesh, especially in the interlock element and in its adjacent areas. Particular care must be taken to define the material characteristics in the regions close to the interlocks. As an assumption, the model adopts different non-linear *BH* magnetization curves for the model zones recognized as undamaged (the larger green part in Fig. 3), partially damaged (in red, and violet in the figure) and fully damaged (in blue). The corresponding *BH* curves have been derived based on catalogue data and previous experiments. The total thickness for the modeled damaged areas is 2 mm, in accordance with the results of previous tests carried out by the authors in relation to the cutting process [9], [23], [24]. Also, different losses per mass unity curves have been used for each of the damaged regions. However, considering the small volume share of the damaged zones compared to the considered fragment, the same frequency-dependent curve could be reasonably used for all the damaged regions when experience-based characteristics are not available. Instead, for those cases where the damaged zones are not negligible, different losses per mass unity curves have to be mandatorily used. It is interesting to observe that during the model tuning, it was noticed that the presence of the three damaged areas in the laminations affect in a not negligible way the value of the Joule losses in the interlock element.

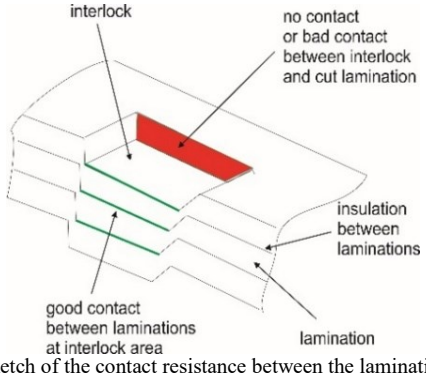

Fig. 4: Sketch of the contact resistance between the lamination sheets in the interlock regions.

Due to the small dimensions of the interlock, it can be considered uniformly affected by damages similar to those that occur during the guillotine cutting. In the developed FEM, the interlock has been considered homogeneously degraded using for this region the same material characteristic considered for the fully damaged zone around the interlock edge.

Figure 4 shows a sketch of three laminations for an interlocked core to highlight the main contact zones between the interlock and the lamination sheets. In the developed model, the insulation between two consecutive sheets in the interlock area has been considered completely degraded, leading to a good electrical contact in axial direction. Hence, an electrical conductivity equal to 1.8 MS/m has been imposed for these regions. The same electrical conductivity value has also been used for the laminated portions that are not affected by the interlock. On the other hand, the portion between the interlock and the lamination edge (the red surface in Fig. 4) has been considered with a bad electrical contact, setting a relatively high value for this specific resistivity in the simulations.

V. Simulation Results by the 3D-FEM Model

This section presents simulation results obtained imposing a sinusoidal flux density in the stator at either 50 Hz and 400 Hz.

A. Flux and eddy current density plots

Figures 5-8 show selected results of the 3D-FEM simulations, considering relatively high contact resistances between the interlocks and lamination (the red surface in Fig. 4). In detail, Fig. 5 shows a sharp reduction of the magnetic flux density in the interlock region. This is caused by the significant eddy currents that circulate because of the good electrical contact between laminations and the interlock area (green surface in Fig. 4). Figures 6-8 display the current density color maps within the interlock and the lamination, showing that the currents induced in the interlock are much higher than those in the lamination. Figure 8 shows these current densities in two different scales to make the current density inside the laminations visible.

B. Iron loss increase due to the interlocks

The adopted solver allows computing the eddy current losses in the interlock and in the lamination sheets, as well as the hysteresis losses. However, the calculation approach used in this research study differs depending on whether the considered lamination area is healthy or damaged by the presence of the interlock.

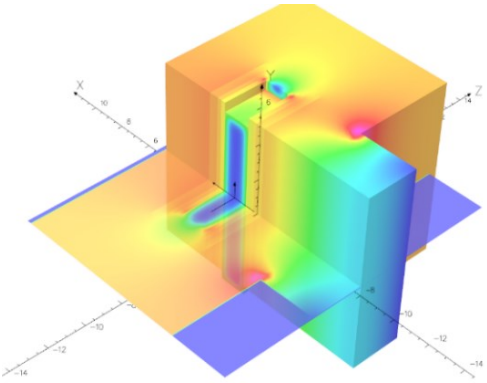
Fig. 5: Flux density distribution at 400 Hz in the considered stator yoke interlocked fragment.

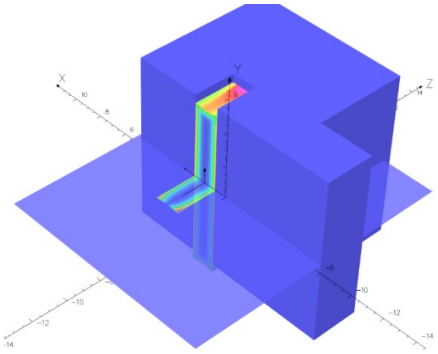
Fig. 6: Current density distribution at 400 Hz in the considered stator yoke interlocked segment.

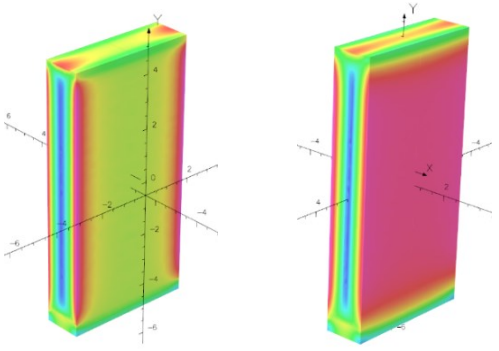
(a) (b)

Fig. 7: Current density distribution inside the interlock region at 400 Hz (a) and at 50 Hz in a different scale to make the phenomenon visible (b).

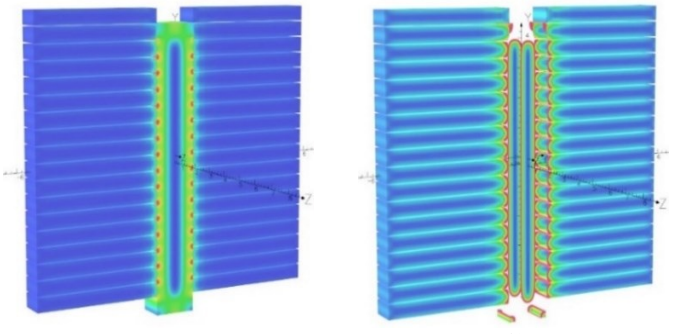
(a) (b)

Fig. 8: Current density distribution in the interlock at 50 Hz for two different scales to make not visible (a) or visible (b) the eddy currents in the laminations.

TABLE I
IRON LOSSES IN THE SIMULATED M270-50A SPECIMENS WITH THE PERCENTAGE INCREASES

Specific losses, (W/kg)	50 Hz		400 Hz	
	1 T (*)	1.53 T (*)	1 T (*)	1.53 T (*)
Without interlocks	1.24 (ref.)	2.60 (ref.)	28.1 (ref.)	64.1 (ref.)
With 3 interlocks	1.31 (+5%)	2.65 (+2%)	30.2 (+7%)	67.5 (+5%)
With 6 interlocks	1.36 (+10%)	2.70 (+4%)	31.1 (+11%)	70.8 (+10%)
With 9 interlocks	1.42 (+14%)	2.76 (+6%)	33.2 (+18%)	74.1 (+16%)

(*): using the guaranteed specific losses (datasheet)
(**): calibrating the catalogue specific losses with the experimental test results.

TABLE II
IRON LOSSES IN THE SIMULATED M400-50A SPECIMENS WITH THE PERCENTAGE INCREASES

Specific losses, (W/kg)	50 Hz		400 Hz			
	1 T (*)	1.52 T (*)	1 T (*)	1 T (**)	1.53 T (*)	1.53 T (**)
Without interlocks	1.81 (ref.)	3.72 (ref.)	42.6 (ref.)	37.9 (ref.)	95.3 (ref.)	84.9 (ref.)
With 3 interlocks	1.92 (+6%)	3.79 (+2%)	44.6 (+5%)	38.9 (+3%)	97.2 (+2%)	86.8 (+2%)
With 6 interlocks	2.04 (+12%)	3.86 (+4%)	45.6 (+7%)	39.6 (+5%)	98.9 (+4%)	88.8 (+4%)
With 9 interlocks	2.08 (+15%)	3.93 (+6%)	46.5 (+9%)	40.6 (+7%)	100.8 (+6%)	90.7 (+7%)

(*): using the guaranteed specific losses (datasheet)
(**): calibrating the catalogue specific losses with the experimental test results

For the healthy zones, conventional procedures have been used for the core losses computation, exploiting the tools available in the used professional FEM package. In detail, hysteresis and eddy current losses are evaluated in each element of the model by a spatial integral based on the peak value of the magnetic flux density over a period in the time domain, and the specific material loss at the specified frequency.

For the three degraded lamination areas around the interlock, the core losses have been initially subdivided into hysteresis and eddy current contributions using the analytical tools integrated into the used FEM package; this computation has been done considering the material as if it were undamaged and using catalogue data. Then, to properly consider the impact of the degradation on the iron losses, the eddy-currents loss contribution has been recalculated considering the Joule losses due to the current distribution predicted by FEM for the degraded material parts. By contrast, the hysteresis losses for the damaged materials have been recalculated considering that, based on the authors' experience, they can be up to four times larger than the losses in the '*green*' magnetic material [9].

Therefore, to consider a gradual deterioration of the material depending on the considered damaged area (see Fig. 3), the hysteresis losses have been increased with respect to the healthy zone by a factor of 1.5 for partially damaged areas, by a factor of 2 for damaged areas and a factor of 3 for fully damaged areas. The same approach based on the separation of eddy-current and hysteresis loss components has been used also for evaluating the losses inside the interlock region.

For the interlock, the material has been considered completely damaged; hence, the hysteresis losses have been increased by a factor of 3 compared to the healthy material. Moreover, with reference to Fig. 4, a perfect electrical contact has been assumed at the green surfaces and infinite contact resistance for the red areas. Therefore, it is expected that the computations will slightly overestimate the iron loss increase compared to measurements on real stator core samples.

The 3D-FEM model shown in Fig. 3 has been solved by imposing the magnetizing current, both for interlock included or not, and obtaining – in this way – also the results for the so-called '*healthy*' fragment. As an example, for the 6 interlocks case, the total losses of the toroidal specimen are computed by combining 21 '*healthy*' areas and 6 areas with the interlock.

For the two magnetic material types under investigation, the losses have been calculated for both 50 Hz and 400 Hz. Table I and Table II report the computed specific losses for the two considered magnetic materials. For M270-50A the simulations have been performed only considering specific losses guaranteed on material datasheet, while for M400-50A simulations have also been done calibrating specific losses curves with experimental data. Looking at these tables, it is possible to conclude that, at 50 Hz, the loss increments due to the interlocking process marginally depend on the material type. For the M400-50A material it has been estimated an increase of the total iron losses at 1.52 T of around 2% for three interlocks (and 4% for 6 and 6% for 9 interlocks), while for the M270-50A material they enlarge by up to 16% at 400 Hz and 1.53 T for 9 interlocks (5% for three interlocks).

It is important to underline that these findings underestimate the experimental results presented in [16] for small interlocked toroidal, having 3 or 6 interlocks as well. Merely, the reason is that in the small toroidal samples used in [16] the linear density of interlocks (defined as the number of interlocks divided by the circumference length at the average diameter) is much higher than that in the tested core samples.

A sensitivity analysis was undertaken to demonstrate that the attempt to consider the damaged materials in areas close to the interlock has little effect on the final results, while it is very important to correctly take into account the insulation damages in the interlock regions. Finally, a measurement-based calibration of the model without interlocks is warmly suggested, because just using the catalogue data the estimation errors can be quite big (e.g., 10% at 400 Hz for this case study, as can be observed from Table II).

VI. EXPERIMENTAL ACTIVITIES

To corroborate the results obtained by numerical simulations on the interlocks impact on magnetic cores, experimental measurements have been conducted on M270-50A and M400-50A stator core samples having different number of interlocks.

Moreover, to assess the repeatability and enhance confidence on the measured quantities, multiple tests have been conducted by two independent laboratories using different equipment and slightly different measurement approaches.

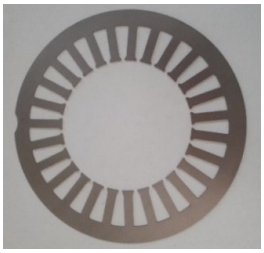

(a)

(b)

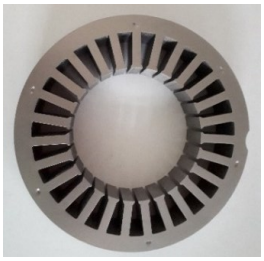

(c)

Fig. 9: (a) Single lamination without interlocks; (b) stator sample with 3 interlocks; (c) and stator core with 6 interlocks.

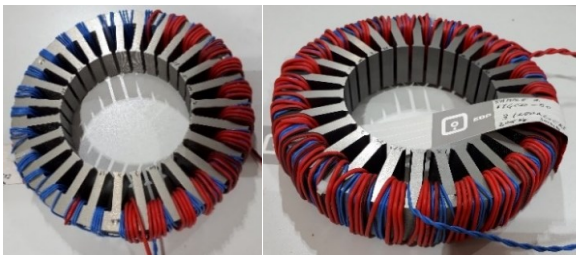

(a) (b)

Fig. 10: (a) Stator sample preparation for the experimental activity, (b) specimen ready for tests (primary winding: red; secondary winding: blue).

It has to be mentioned that the two laboratories tested different samples. However, all samples with same material grade have been produced at the same time, using the same production process and the same raw material. Therefore, the results on different samples can be effectively compared to assess the impact of interlocks on the stator core losses.

A. Sample preparation

Figure 9 shows the specimens for this research activity. In detail, Fig. 9a shows a single lamination sheet for the sample without interlocks; in this case the lamination sheets have been tightened together with plastic strips to form the complete stator core sample for measurements. Figure 9b and Fig. 9c show the sample cores with three and six interlocks, respectively. To perform magnetic and energetic performance evaluations, ring core measurements have been done applying two windings for each sample, as shown in Fig. 10. When the primary/magnetizing winding is supplied by an alternating voltage, it produces an alternating magnetic field inside the stator yoke, according to Ampere's circuital law. This field in turn results in a magnetic flux that induces a voltage at the terminals of the measuring/sensing winding. In linear magnetic conditions, the induced voltage does not present significant distortions compared to the excitation waveform; for a pure sinusoidal excitation this results in a form factor (defined as the ratio between the rms value and the rectified mean value of the voltage) equal to 1.11.

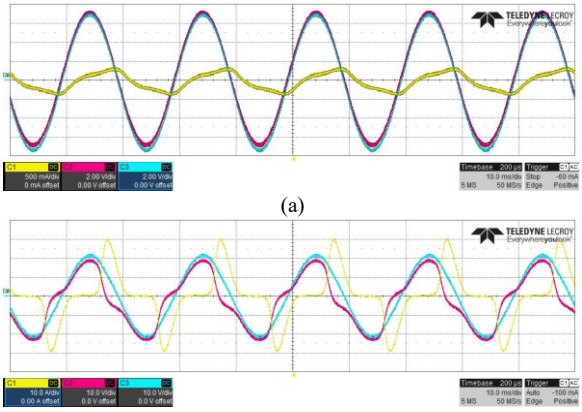

(a)

(b)

Fig. 11: Primary (cyan) and secondary (purple) voltages and current (yellow) waveforms during tests at 50 Hz on a M400-50A sample: measurements points at low voltage (a) and high voltage (b) values.

The higher the considered magnetic field, the higher is the effect of nonlinearities on the induced voltage at the secondary winding. In fact, when the magnetic material saturates, the absorbed primary current is highly distorted. As a consequence, the induced voltage on the secondary winding is also distorted and its form factor drifts away. This effect is well visible in Fig. 11 that shows the absorbed current, the primary and secondary voltages for one M400-50A sample tested at 50 Hz, both at low voltage (not saturated magnetic core) and high voltage (saturated magnetic core) conditions.

B. Lab#1 test rig description

Figure 12 illustrates the measurement setup used in the first laboratory (lab#1). The equipment consists of an 18 kVA *ac* linear power source that can produce a pure sinusoidal voltage in the range 20Hz – 5kHz, and a high-precision power meter that measures the current absorbed by the primary winding and the voltage induced in the secondary one. In this way, the Joule losses on the primary winding do not affect the measurements. The oscilloscope is mainly used for monitoring the peak value of the magnetizing current to avoid damages at the power meter when highly distorted currents are absorbed.

C. Lab#2 test rig description

Figure 13 sketches the measurement setup used in the second laboratory (lab#2). The setup mainly consists of a linear power amplifier, a measurement amplifier, and a data acquisition system (DAQ) interfaced with a PC. The power amplifier in use allows for a continuous power of 1kVA, with a short time peak power of 2kVA, and exhibits a frequency bandwidth of DC to 30kHz.

The primary current is measured utilizing a shunt resistor. In this case a non-inductive shunt resistor is used to avoid any phase shifts in the measured current, and therefore to prevent an error in the characterization of the associated core losses [25]. Measuring amplifiers in the DAQ system amplify the respective signals of the primary current and the induced secondary voltage, and an iterative in-house developed learning control is used to guarantee either a sinusoidal magnetic flux density or sinusoidal field strength within the form factor range specified in the corresponding IEC standard [21], [26].

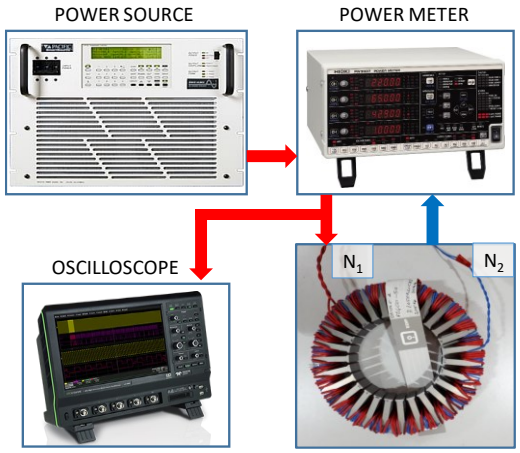

Fig. 12: Sketch of the measurement setup used in lab#1 (red arrows: current path; blue arrow: voltage measurement).

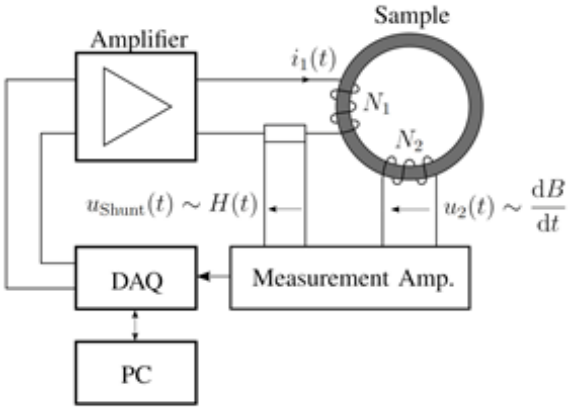

Fig. 13: Sketch of the measurement setup used in lab#2.

D. *Measurement data elaboration*

Assuming that no minor loops are present in the main hysteresis loop, the peak value of the magnetic flux in the stator yoke of the sample can be computed by (1):

$$\Phi = \frac{|\bar{V}_2|}{4fN_2} \tag{1}$$

where $|\bar{V}_2|$ is the rectified mean value of the voltage induced at the secondary winding, N_2 is the number of turns of the secondary winding and f is the frequency of the excitation voltage. Then, the magnetic flux density B can be computed by (2), where A is the cross-section area of the stator yoke.

$$\mathrm{B} = \frac{\Phi}{A} \tag{2}$$

By the measured peak value of the current that flows in the primary winding I_1 and the average length of the yoke circumference l, the magnetic field H can be computed by (3), where N_1 is the number of turns for the primary winding.

$$\mathrm{H} = \frac{N_1 I_1}{l} \tag{3}$$

Taking the measured B- and H- values, the experimental BH magnetization curve for the material of the samples can be obtained. To avoid the influence of the Joule losses in the primary winding, the iron losses within the magnetic material can be computed by (4), where the excitation current and the induced voltage are measured simultaneously by the power meter.

$$P_{Fe} = \frac{N_1}{N_2}\frac{1}{T}\int_0^T i_1(t)v_2(t)dt \tag{4}$$

Since the primary winding is closely wound around the stator yoke, the magnetic flux as well as the iron losses obtained are located inside the stator yoke. Therefore, the material specific losses are evaluated by (5), where m is the mass of the yoke for the considered sample.

$$p_{Fe} = \frac{P_{Fe}}{m} \tag{5}$$

It has to be highlighted that when the magnetic material starts saturating, the magnetic flux is not only located along the samples yoke but tends to extend into the tooth roots [11], [27]. However, this effect does not impact the comparative analyses, as it exists with similar extent both in the experimental activity and the simulations.

Furthermore, even if the two independent laboratories used slightly different measurement setups and equipment, their acquired quantities have been post-elaborated in the same way according to the above describe approach.

E. *Experimental results and simulation validation*

The validation of the simulation results has been done by measuring in each laboratory three stator samples made of M270-50A and three stator samples made of M400-50A. For each magnetic material, the three samples differ with regard to the number of interlocks in the lamination, specifically zero, three, or six interlocks, respectively. The weight and the geometrical dimensions of each specimen have been accurately measured for a precise evaluation of the yoke cross section area and mass. Then, all the samples have been wound with 108 turns both for the magnetizing and the sensing windings, such that $N_1 = N_2$.

In lab#1, the measurements have been done applying pure sinusoidal voltages at different frequencies in the range 50Hz – 400Hz and for magnetic field values up to 2000 A/m. Beyond this value, the form factor of the induced voltage was higher than 1.14, particularly at low frequency; hence, the measurements have been no longer considered as valid.

In lab#2, the same frequency and magnetic field ranges have been investigated imposing a controlled primary voltage that guarantees a sinusoidal magnetic flux density in the sample. Therefore, in this case the form factor intrinsically does not vary significantly with respect to the reference value of 1.11.

Figure 14 shows the BH magnetization curve measured at 50 Hz for the M270-50A samples without interlocks. While the values measured by the two laboratories well match, they differ from catalogue data, as expected particularly in the '*knee*' region. This is due to the lamination production process that negatively impacts on the magnetic material characteristics [5], [6], [9].

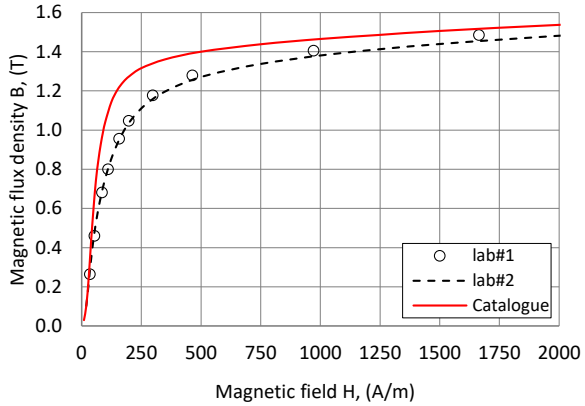

Fig. 14: *BH* curves measured for M270-50A samples without interlocks and material catalogue data at 50 Hz.

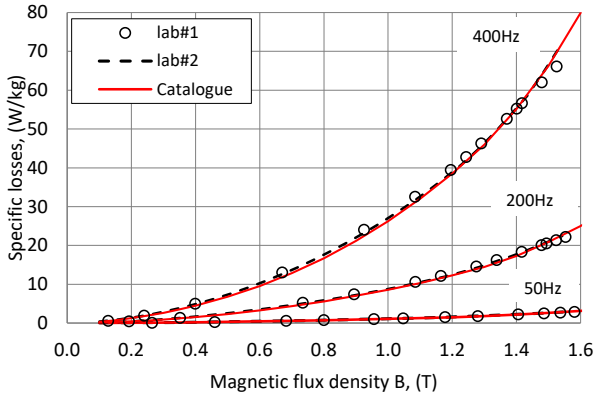

Fig. 15: Specific core losses curves measured at different frequencies for M270-50A samples without interlocks and material catalogue data.

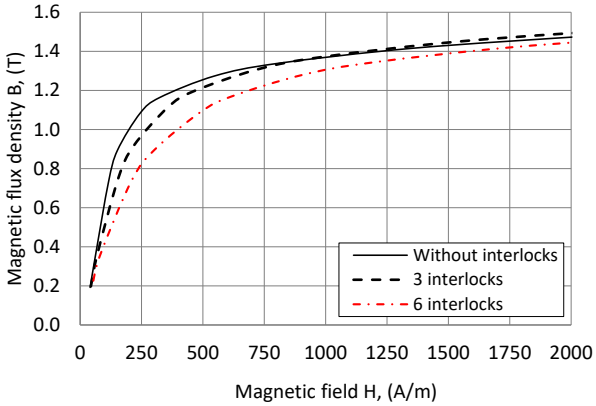

Fig. 16: *BH* curves measured for the three M270-50A samples at 200 Hz.

For each sample, similar curves measured at other frequency levels resulted substantially overlapped to those shown in the figure. The specific losses versus the magnetic flux density for the M270-50A samples without interlocks at 50 Hz, 200 Hz and 400 Hz are shown in Fig. 15. Again, the values measured by the two laboratories well overlaps as well as with those reported on material catalogue.

Figure 16 compares magnetization curves measured at 200 Hz for the M270-50A samples with different number of interlocks. This comparison clearly reveals, particularly in the knee region, the additional material degradation when interlocks are used to packet the lamination sheets, confirming results also obtained by other research works on the topic [13].

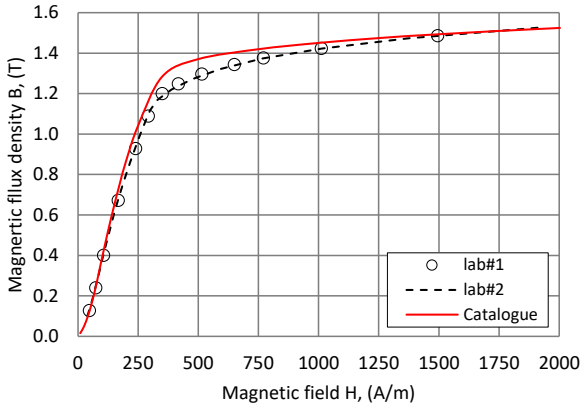

Fig. 17: *BH* curves measured for M400-50A samples without interlocks and material catalogue data at 400 Hz.

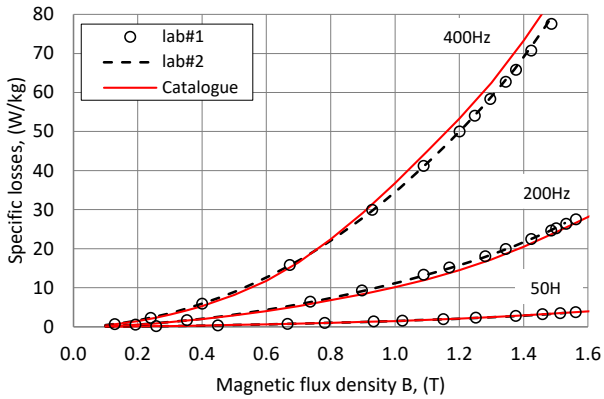

Fig. 18: Specific core losses curves measured at different frequencies for M400-50A samples without interlocks and material catalogue data.

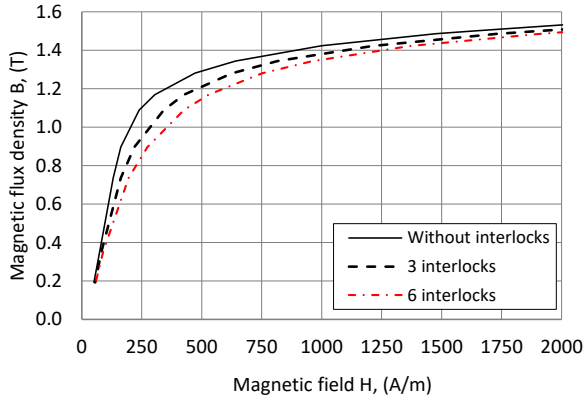

Fig. 19: *BH* curves measured for the three M400-50A samples at 200 Hz.

Similar comparisons are reported in Figs. 17-19 for the M400-50A material samples. Also in this case, laboratory measurements and catalogue data are in good agreement regarding the specific loss curves at different frequencies (Fig. 18). Moreover, measurement results shown in Fig. 17 and Fig. 19 again confirm the negative impact on magnetic material characteristics when interlocks are used to packet the lamination sheets. To compare the interlocks impact on magnetic material losses predicted by the conducted FEM analyses, Figs. 20-23 report for the two investigated materials the specific losses measured at 50 Hz and 400Hz versus the magnetic flux density. These plots show that the higher the number of interlocks, the higher is the impact on the iron losses, particularly at high magnetic flux density levels.

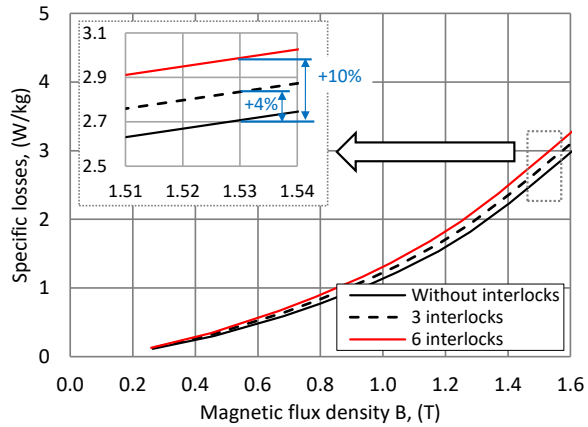

Fig. 20: Core losses measured for the three M270-50A samples at 50 Hz.

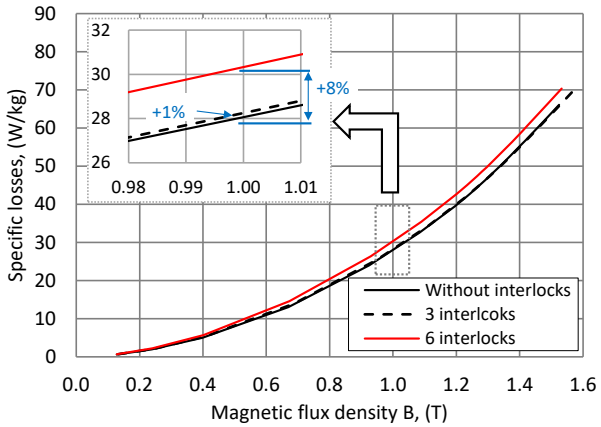

Fig. 21: Core losses measured for the three M270-50A samples at 400 Hz.

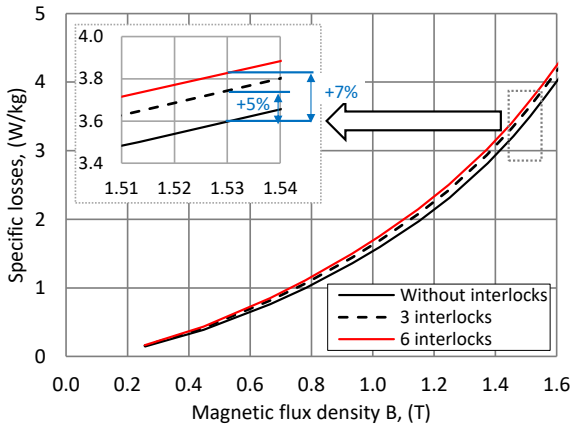

Fig. 22: Core losses measured for the three M400-50A samples at 50 Hz.

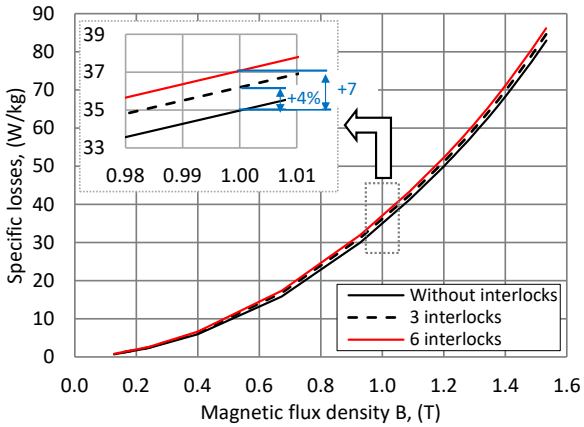

Fig. 23: Core losses measured for the three M400-50A samples at 400 Hz.

TABLE III
COMPARISON BETWEEN SIMULATED AND MEASURED IRON LOSSES FOR THE M270-50A SPECIMENS

Specific losses, (W/kg)	50 Hz				400 Hz			
	1 T		1.53 T		1 T		1.53 T	
	Sim	Meas	Sim	Meas	Sim	Meas	Sim	Meas
Without interlocks	1.24	1.14	2.60	2.71	28.1	28.1	64.1	66.5
With 3 interlocks	1.31	1.22	2.65	2.83	30.2	28.3	67.5	66.3
With 6 interlocks	1.36	1.31	2.70	2.99	31.1	30.3	70.8	70.2

TABLE IV
COMPARISON BETWEEN SIMULATED AND MEASURED IRON LOSSES FOR THE M400-50A SPECIMENS

Specific losses, (W/kg)	50 Hz				400 Hz			
	1 T		1.53 T		1 T		1.53 T	
	Sim	Meas	Sim	Meas	Sim	Meas	Sim	Meas
Without interlocks	1.81	1.53	3.72	3.52	37.9	34.8	84.9	82.2
With 3 interlocks	1.92	1.63	3.79	3.69	38.9	36.2	86.8	84.3
With 6 interlocks	2.04	1.69	3.86	3.78	39.6	37.1	88.8	86.0

However, focusing on the measurements conducted at 400Hz, where the absolute power values are in the order of tens of Watt, the results for the investigated samples show that the use of 3 interlocks marginally impact the measured M270-50A cores, while the use of 6 interlocks present a more evident increase on the iron losses for the cores made by both materials. The zoomed areas on the figures show the percentage increase when three and six interlocks are applied with respect to the sample without interlocks. Table III and Table IV list for the M270-50A and M400-50A specimens the specific losses measured at defined flux density values, together with the values predicted by the FEM simulations. Roughly comparing the data, the measured specific loss values and the percentage increases slightly differ with those predicted by the numerical analyses. This is mainly imputed to the small power values associated to the phenomena under investigation.

In fact, multiple measurement repetitions on the same sample may provide slightly different values [1]. However, all the measurements conducted by the two independent laboratories on the samples under investigation provided similar results and, in general, the measured percentage trends agree with those predicted by the numerical analyses. It is also interesting to note that the percentage increase in the core losses measured for the M400-50A samples well agree with the simulation results obtained calibrating the catalogue specific losses with experimental test results (see Table II). It is therefore reasonable to consider the developed 3D-FEM model for a satisfactorily accurate prediction of the magnetic material losses for the modeled samples. However, an initial measurement-based calibration of the magnetic material characteristics, both for the *BH* magnetization curve and for the specific core losses is suggested.

VII. Conclusion

This paper proposed an original approach for the numerical modeling of the electromagnetic phenomena interlocked stator cores. A 3D-FEM model has been introduced to approach the problem, considering the material degradation around the dowels through layered regions with different magnetic material characteristics. The modeling novelties are on the assumed electrical conductivity for the conductive paths for the eddy currents, as well as the approach used to compute the hysteresis and eddy-current losses in the degraded areas of the magnetic material. The impact of the interlocks predicted by the numerical analyses has been validated through interlaboratory measurements on different M270-50A and M400-50A stator core samples with zero, three and six interlocks at the average diameter of the stator yoke. For the considered stator cores, wound as toroidal samples, the measurements revealed an impact of the interlocks of some percent on the core losses, at least for the considered geometries, materials, and used punching and stacking technologies. However, their impact on the *BH* magnetization curves seems more evident. The 3D-FEM model provided a good estimation of the loss increments due to the presence of the interlocks, particularly when experimentally calibrated data are considered for the magnetic material.

The study has been conducted for a circumferential magnetic flux in the stator yoke, leaving aside the potential impact of the interlocks on the creation of flux loops when rotating magnetic fields are applied to the stator core. However, the here presented findings, together with the developed modeling approach, pave the way for future studies regarding the impact of rectangular dowels, also positioned in different parts of the stator core (e.g., radially oriented interlocks stamped into the stator teeth), as well as when considering different orientations. It is expected that linked magnetic fluxes around the interlocks can impact the magnetic material losses.

Acknowledgments

This work has been supported by the COMET-K2 "Center for Symbiotic Mechatronics" of the Linz Center of Mechatronics (LCM) funded by the Austrian federal government and the federal state of Upper Austria.

References

[1] Z. Gmyrek, A. Cavagnino, S. Vaschetto, and G. Bramerdorfer, "Loss Modeling for Interlocked Magnetic Cores", in Proc. IEEE Energy Convers. Congr. Expo., Detroit, MI, USA, 2020, pp. 1060–1066.

[2] P. A. Hargreaves, B. C. Mecrow, and R. Hall, "Calculation of iron loss in electrical generators using finite element analysis," *IEEE Trans. Ind. Appl.*, vol. 48, no. 5, pp. 1460–1466, Sep./Oct. 2012.

[3] C. Dobler, D. Wockinger, G. Bramerdorfer, G. Goldbeck, and W. Amrhein, "Studies of Measurement Uncertainties in the Characterization of Soft Magnetic Materials and their Impact on the Electric Machine Performance Prediction" in *Proc. IEEE Energy Convers. Congr. Expo.*, Vancouver, CA, 2021, pp. 4411–4417.

[4] G. Bramerdorfer, M. Kitzberger, D. Wockinger, B. Koprivica, and S. Zurek, "State-of-the-art and future trends in soft magnetic materials characterization with focus on electric machine design – part 2," *tm - Technisches Messen*, vol. 86, no. 10, pp. 553-565, Oct. 2019. [Online]. www.degruyter.com/view/journals/teme/86/10/article-p553.xml.

[5] M. Bali, H. De Gersem, and A. Muetze, "Determination of original nondegraded and fully degraded magnetic characteristics of material subjected to laser cutting," *IEEE Trans. Ind. Appl.*, vol. 53, no. 5, pp. 4242–4251, Sep./Oct. 2017.

[6] W. Wilczynski, A. Schoppa, and J. Schneider, "Influence of the different fabrication steps of magnetic cores on their magnetic properties," *Electr. Rev.*, vol. R.80, no. 2, pp. 118–120, 2004.

[7] A. Schoppa, J. Schneider, C.-D. Wuppermann, and T. Bakon, "Influence of welding and sticking of laminations on the magnetic properties of non-oriented electrical steels", in *Journal of Magnetism and Magnetic Materials*, 2003, pp. 367–369.

[8] A. Krings, S. Nategh, O. Wallmark, and J. Soulard, "Influence of the welding process on the magnetic properties of a slot-less permanent magnet synchronous machine stator core", in 2012 XXth International Conference on Electrical Machines, Sep. 2012, pp. 1333–1338.

[9] Z. Gmyrek, and A. Cavagnino, "Influence of Punching, Welding, and Clamping on Magnetic Cores of Fractional KiloWatt Motors", *IEEE Trans. Ind. Appl.*, Vol. 54, No. 5, pp. 4123-4132, Sept./Oct. 2015.

[10] K. Bourchas, A. Stening, J. Soulard, A. Broddefalk, M. Lindenmo, M. Dahlen, and F. Gyllensten, "Quantifying Effects of Cutting and Welding on Magnetic Properties of Electrical Steels", *IEEE Trans. Ind. Appl.*, vol. 53, no. 5, pp. 4269–4278, Sep. 2017.

[11] M. Cossale, A. Krings, J. Soulard, A. Boglietti, and A. Cavagnino, "Practical Investigations on Cobalt-Iron Laminations for Electrical Machines", *IEEE Trans. Ind. Appl.*, Vol. 51, No. 4, pp. 2933-2939, Jul./Aug. 2015.

[12] E. Lamprecht, M. Hömme, and T. Albrecht, "Investigations of Eddy Current Losses in Laminated Cores Due to the Impact of Various Stacking Processes," in Conf. rec. 2nd Inter. Electric Drives Production Conf., pp. 1-8, 2012.

[13] S. Imamori, S. Steentjes, and K. Hameyer, "Influence of Interlocking on Magnetic Properties of Electrical Steel Laminations," *IEEE Trans. Magnetics*, Vol. 53, No. 11, November 2017.

[14] Li-Hsiang Liu, and Lee-Cheng Liu, "Analysis of interlocking performances on non-oriented electrical steels," *AIP Advances* 8, 056605 (2018); https://doi.org/10.1063/1.5005071.

[15] Gui-Yu Zhou, He Hao, Meng-Jia Jin, and Jian-Xin Shen, "Influence of interlocking dowels on motor core loss," *COMPEL*, Vol. 35, pp. 808-820, 2016.

[16] K. Senda, H. Toda, and M.Kawano, "Influence on Interlocking on Core Magnetic Properties," *IEEJ Journal of Industry Apllications*, Vol. 4,No. 4, pp. 496-502, 2015.

[17] G. Bramerdorfer, M. Kitzberger, D. Wockinger, B. Koprivica, and S. Zurek, "State-of-the-art and future trends in soft magnetic materials characterization with focus on electric machine design – part 1," *tm - Technisches Messen*, vol. 86, no. 10, pp.540 – 552, Oct. 2019. [Online]: www.degruyter.com/view/journals/teme/86/10/article-p540.xml.

[18] T. Nakayama, and H. Kojima, "Interlocking Performances on Non-Oriented Electrical Steels," *JMEPEG* (2007) 16:7–11.

[19] S. Sprague, "An Assessment of Common Core Assembly Methods for Thin Gauge Non-Oriented Electrical Steels", in Conf. Rec. WMM'16 (Lecture 11), Rome, Italy, pp.1-19, 2016.

[20] Heng-Sheng Lin, Ho-ChungFu, Li-HsiangLiu, and Yun-KuiHuang, De-HuaFang "Stacking with cylindrical spots in lamination of stamped electrical steel sheets," in *Proc. Eng.*, Vol. 207, pp.992-997, 2017.

[21] *IEC 60404-6, Magnetic Materials – Part 6: Methods of measurement of the magnetic properties of magnetically soft metallic and powder materials at frequencies in the range 20Hz to 100kHz by the use of ring specimens,* Int. Electrotechnical Comm. Std. Second edition, May 2018.

[22] S. Xue, W.Q. Chu, Z.Q. Zhu, J. Peng, S. Guo, and J. Feng, "Iron loss calculation considering temperature influence in non-oriented steel laminations", *IET Sci. Meas. Technol.*, 2016,Vol. 10, Iss. 8, pp. 846-854.

[23] Z. Gmyrek, A. Cavagnino, "Analytical Model of the Ferromagnetic Properties in Laminations Damaged by Cutting", in Proc. IEEE Energy Convers. Congr. Expo., Vancouver, BC, Canada, 2021, pp. 4000–4007.

[24] M. Dems, Z. Gmyrek and K. Komeza, "Analytical Model of an Induction Motor Taking into Account the Punching Process Influence on the Material Properties' Change of Lamination", *Energies* 2021, 14(9), 2459.

[25] K. Trnka, and R. Werner, "Compensation of the frequency-dependent error in current measurement in the determination of magnetization characteristics and losses", in *tm – Technisches Messen 2018; 85(10),* pp. 591–601, 2018.

[26] D. Andessner, R. Kobler, J. Passenbrunner, and W. Amrhein, "Measurement of the Magnetic Characteristics of Soft Magnetic Materials with the Use of an Iterative Learning Control Algorithm, " in *2011 IEEE Vehicle Power and Propulsion Conf.* , IEEE, 2011, pp.1-6.

[27] A.J. Clerc, and A. Muetze, "Measurement of stator core magnetic degradation during the manufacturing process", *IEEE Trans. Ind. Appl.*, Vol. 48, No. 4, pp. 1344-1352, Jul./Aug. 2012.

Silvio Vaschetto (S'10–M'13–SM'19) received the M.Sc. and Ph.D. degrees in electrical engineering from the Politecnico di Torino, Italy, in 2007 and 2011, respectively. He then joined ABB IEC LV Motors Technology Center, Vittuone, Italy as R&D engineer. From 2012 to 2014 he was with Magna Electronics Italy, as Electromagnetic Simulation and Motor Design Engineer. He is currently an Associate Professor at the Energy Department "G. Ferraris", Politecnico di Torino. His research interests include electromagnetic design, thermal design, and energetic behavior of electrical machines for high-performance applications. Prof. Vaschetto is Associate Editor for IEEE TRANSACTIONS ON INDUSTRY APPLICATIONS and for *IET Electric Power Applications*.

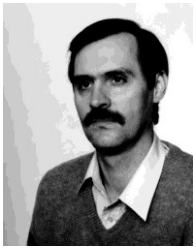

Zbigniew Gmyrek received the Ph.D. and D.Sc. degrees in electrical engineering from the Lodz University of Technology (LUT), Łódź, Poland, in 1996 and 2006, respectively. He is currently an Associate Professor with the Institute of Mechatronics and Information Systems, LUT, Poland. He is the Author of 140 scientific papers. His research interests include magnetic material modeling and measuring, and studying the impact of mechanical cut on the magnetic material properties. Prof. Gmyrek is a Reviewer of many scientific journals, including the IEEE TRANSACTIONS ON INDUSTRY APPLICATIONS, IEEE TRANSACTIONS ON INDUSTRIAL ELECTRONICS, IEEE TRANSACTIONS ON MAGNETICS, *IET Electric Power Applications*, and *Sensors*. He was Guest Editor of Special Section for *Energies*.

Christoph Dobler, born in Innsbruck 1991. After receiving his BSc in Mechatronics from the Leopold-Franzens-University Innsbruck, his studies continued in Linz, where he received his Dipl.-Ing. (MSc) from the Johannes Kepler University (JKU). Since 2019 he is working part-time at the Institute for Electrical Drives and Power Electronics at the JKU, and since Dec. 2020 full-time as a University Assistant at said Institute. Since 2021 he is enrolled in the Dr. Tech. (PhD) program at the JKU. His main research interests include the characterization and modeling of magnetic materials, with the focus on soft magnetic components.

Gerd Bramerdorfer (S'10-M'14-SM'18) received the PhD degree in Electrical Engineering in 2014 from Johannes Kepler University Linz, Austria. He is an Associate Professor with the Faculty of Engineering and Natural Sciences, Johannes Kepler University Linz, and a Key Researcher for the Linz Center of Mechatronics, Austria. His research interests include the design, modeling, and optimization of high-performance electric machines and drives. Dr. Bramerdorfer is a Senior Member of IEEE, an Associate Editor of the IEEE TRANSACTIONS ON ENERGY CONVERSION, and a past Associate Editor of the IEEE TRANSACTIONS ON INDUSTRIAL ELECTRONICS. He is a reviewer for international journals and conferences.

Andrea Cavagnino (M'04–SM'10–F'20) was born in Asti, Italy, in 1970. He received his M.Sc. and Ph.D. degrees in electrical engineering from the Politecnico di Torino, Italy, in 1995 and 2000, respectively. He is a professor at the Politecnico di Torino. He has authored or co-authored more than 250 papers, receiving four Best Paper Awards. His research interests include electromagnetic design, thermal design, and energetic behaviour of electrical machines. He usually cooperates with factories for a direct technological transfer and he has been involved in several public and private research projects. Prof. Cavagnino is an Associate Editor of the IEEE TRANSACTIONS ON ENERGY CONVERSION (TEC), a Past Chair of the Electrical Machines Technical Committee of the IEEE Industrial Electronics Society, a past Associate Editor of the IEEE TRANSACTIONS ON INDUSTRIAL ELECTRONICS (TIE), and the IEEE TRANSACTIONS ON INDUSTRY APPLICATIONS. He was also a Guest Editor of six Special Sections for IEEE-TIE and co-Editor in Chief of a Special Issue for IEEE-TEC. Prof. Cavagnino was a technical program chair of the IEEE-IEMDC 2015 and IEEE-ECCE 2022 conferences. He is a reviewer for several IEEE TRANSACTIONS and other international journals and conferences.